Research Article Vol. 28, No. 3 / 3 February 2020 / Optics Express 3745
Optics EXPRESS

Design and experimental demonstration of Doppler cloak from spatiotemporally modulated metamaterials based on rotational Doppler effect

BAIYANG LIU,[1] HENRY GIDDENS,[2] YIN LI,[1] YEJUN HE,[1] SAI-WAI WONG,[1,3] AND YANG HAO[2,4]

[1]College of Electronics and Information Engineering, Shenzhen University, Shenzhen, 518061, China
[2]School of Electronics Engineering and Computer Science, Queen Mary University of London, London, E1 4NS, UK
[3]wongsaiwai@ieee.org
[4]y.hao@qmul.ac.uk

Abstract: Recently, spatiotemporally modulated metamaterial has been theoretically demonstrated for the design of Doppler cloak, a technique used to cloak the motion of moving objects from the observer by compensating for the Doppler shift. Linear Doppler effect has an angular counterpart, i.e., the rotational Doppler effect, which can be observed by the orbital angular momentum (OAM) of light scattered from a spinning object. In this work, we predict that the spatiotemporally modulated metamaterial has its angular equivalent phenomenon. We therefore propose a technique to observe the rotational Doppler effect by cylindrical spatiotemporally modulated metamaterial. Conversely, such a metamaterial is able to cloak the Doppler shift associated with linear motion by generating an opposite rotational Doppler shift. This novel concept is theoretically analyzed, and a conceptual design by spatiotemporally modulating the permittivity of a voltage-controlled OAM ferroelectric reflector is demonstrated by theoretical calculation and numerical simulation. Finally, a Doppler cloak is experimentally demonstrated by a spinning OAM metasurface in radar system, which the spatiotemporal reflection phase are mechanically modulated. Our work presented in this paper may pave the way for new directions of OAM carrying beams and science of cloaking, and also explore the potential applications of tunable materials and metasurfaces.

1. Introduction

The possibility of cloaking an object from detection by an external observer has recently become a topic of considerable interest [1,2]. Such invisibility cloaks can be designed explicitly by transformation optics, in which a conformal coordinate transformation is applied to Maxwell's Eq. [3,4]. For a restricted bandwidth, using the freedom of design that passive metamaterials provide, one can redirect the electromagnetic fields to obtain a spatial distribution that defines the cloak. However, the visibility of the cloaks can be detected by observation of the Doppler effect when in relativistic motion [5]. In particular, the Doppler frequency shift, which arises from the relativistic motion, may shift the wave outside the cloaking bandwidth, thus the cloak becomes detectable. The possibility to cloak the motion of objects from a static observer has recently been discussed [6]. A moving object is enveloped with a spatiotemporally modulated metamaterial which is able to generate an opposite frequency shift to the one of linear Doppler effect. The resulting composite system can appear to a Doppler radar as stationary when it is in fact moving. In addition, as a 2-dimentional metamaterial, a time-varying metasurface with proper time-dependent transmission coefficient has also been discussed for realization of the Doppler cloak [7–9]. The Doppler effect firstly described in 1842 is a well-known phenomenon

#382700 https://doi.org/10.1364/OE.382700
Journal © 2020 Received 8 Nov 2019; revised 19 Dec 2019; accepted 15 Jan 2020; published 27 Jan 2020

Optics EXPRESS

in which the relativistic motion between a source and an observer causes a frequency shift in reflected light waves. However, the rotational Doppler effect of OAM waves scattered by a spinning target is less well-known [10–14]. In an OAM beam, the momentum has a rotating component at every position within the beam. The rotational Doppler effect is generated by the azimuthal component of the momentum and relative rotational motion. In other words, the rotational Doppler effect is the transformation of Doppler effect into cylindrical coordinates. Metasurfaces covering the phase change range from 0 to 2π can be designed as an OAM generator known as OAM metasurface [15]. Recently, the rotational Doppler effect by a spinning OAM metasurface has been experimentally observed. The spinning motion of an OAM metasurface modulates the reflection phase spatiotemporally causing rotational Doppler shift [16,17].

In this paper, inspired by the spatiotemporally modulated metamaterial that can generate Doppler shift, we explore the angular equivalent phenomenon of such a metamaterial. Here we transform the spatiotemporally modulated metamaterial from the Cartesian coordinate to a cylindrical coordinate, an angular counterpart phenomenon is predicted. Based on spatiotemporally modulating the artificial permittivity of the material in azimuthal angle, i.e., in a cylindrical coordinate, the reflection phase of the waves can be modulated in order to mimic the spinning motion. Thus we can generate an OAM beam with rotational Doppler effect from a stationary slab via electrically modulating the permittivity of the material. Moreover, we explore the potential applications of rotational Doppler effect from spinning OAM metasurface, we demonstrate the Doppler cloak concept by an OAM metasurface with both linear moving and spinning in Doppler radar system, a zero-frequency shift is experimentally observed. It means that the Doppler radar detects the OAM metasurface as stationary but the fact that it is moving.

The paper is organized as follow: Firstly, we outline the fundamental theory of spatiotemporally modulated metamaterial in a cylindrical coordinate for observation of rotational Doppler effect. Subsequently, a conceptual design is proposed to demonstrate this concept. Specifically, a voltage-controlled OAM reflector based on ferroelectric materials with relative permittivity which is spatiotemporally modulated by applying a bias voltage. To some extent, our design combines the concept of OAM generation and time-modulated array [18,19]. The material parameters are based on measured dielectric tunability from Barium-Strontium Titanate ceramics at microwave frequency, and theoretical and simulation results demonstrate the rotational Doppler effect for Doppler cloak. Finally, as a 2-dimentional case of spatiotemporally modulated metamaterial, a spinning OAM metasurface mechanically modulate the spatiotemporal reflection phase is used to experimentally demonstrate the Doppler cloak concept. Different from the time-varying metasurface generating linear Doppler effect [7–9], the proposed cylindrical spatiotemporally modulated metamaterial generating OAM beam with rotational Doppler effect can mimic the motion spinning, which may find more applications for detection of spinning objects. The proposed approach is expected to broaden the applications of OAM carrying beams, explores the potential application of ferroelectric materials and metasurfaces, and promises important advantages in scenarios such as Doppler cloak, Doppler radar deception and Doppler cancellation in wireless communication [20].

2. Theoretical analysis

A way to achieve the Doppler shift from a spatiotemporally modulated metamaterial was recently discussed [6]. The space-time permittivity $\epsilon_r(z,t)$ is modulated according to the travelling wave-profile in the Cartesian coordinate $\epsilon_r(z,t) = \epsilon_{r_0} + \delta\epsilon cos(\omega_m t + k_m z)$, where the $\omega_m = 2\pi f_m$ is the modulation frequency, as shown in Fig. 1(a). The modulated permittivity introduces two time-varying phase shift $exp(\pm j\omega_m t)$ to the reflected waves. By the Fourier transform, the phase varying in time domain corresponds to a frequency shift $\Delta f = \pm\omega_m/2\pi$ measured in Hz. On the other hand, the Doppler effect has its angular equivalent, i.e., the rotational Doppler effect [10–14], which can be observed from a spinning OAM beam leading to a time-varying phase

Optics EXPRESS

$\varphi(\theta, t)$ in cylindrical coordinates [16]. The following Eq. shows the spatiotemporally modulated reflection phase of a spinning OAM beam.

$$\varphi(\theta, t) = \theta l - 2\pi l f_m t \tag{1}$$

where θ is the azimuthal angle, l is the OAM mode and f_m is the spinning frequency. The first term θl defines the mode of OAM beam, and the second term $-2\pi l f_m t$ defines the spinning motion in $+\theta$ direction. Similarly, we can spatiotemporally modulate the permittivity in azimuthal direction $\epsilon_r(\theta, t)$, and introduce a corresponding space-time-varying phase shift $\varphi(\theta, t)$ consistent with Eq. (1), the one of rotational Doppler effect from a spinning OAM beam. The proposed spatiotemporally modulated metamaterial is shown in Fig. 1(b). Let us denote the thickness of the metamaterial as d and the wavelength of the incident wave as λ, the reflection phase of such reflector is given by

$$\varphi = \frac{4\pi d\sqrt{\epsilon_r}}{\lambda} \tag{2}$$

By matching Eqs. (1) and (2) we can define a spatiotemporal permittivity of the metamaterial as the following Eq.

$$\sqrt{\epsilon_r(\theta, t)} = \frac{\lambda(\theta l - 2\pi l f_m t)}{4\pi d} \tag{3}$$

This spatiotemporal permittivity condition describes the phase variation matched with that of the rotational Doppler effect from a spinning OAM beam, which generates a rotational Doppler frequency shift [10,16]

$$\Delta f = \frac{l\Omega}{2\pi} = l f_m \tag{4}$$

In our case only a positive frequency shift is obtained, because the modulated permittivity $\epsilon_r(\theta, t)$ is a monotonic function varying with time. The travelling-wave profile of the modulated permittivity and spinning reflection phase are shown in Figs. 2(a) and 2(b), respectively.

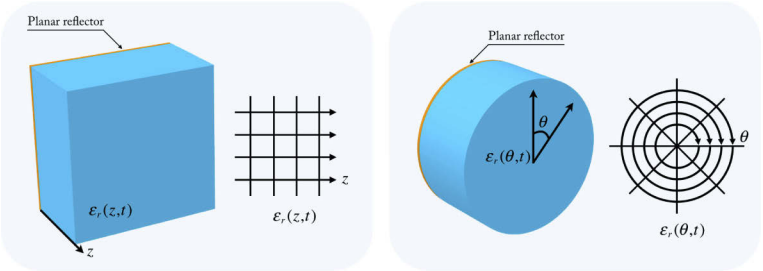

(a) (b)

Fig. 1. (a) Planar reflector loaded with a spatiotemporally modulated metamaterial, the artificial permittivity $\epsilon_r(z, t)$ is modulated in z axis of Cartesian coordinate corresponding to linear Doppler effect. (b) The proposed planar reflector loaded with a cylindrical spatiotemporally modulated metamaterial, the artificial permittivity $\epsilon_r(\theta, t)$ is modulated in angular direction θ and introduces a space-time-varying reflection phase $\varphi(\theta, t)$ corresponding to rotational Doppler effect from a spinning OAM beam.

3. Electrical modulation: Doppler cloak by ferroelectric materials

3.1. *Full 2π reflection phase tuning ferroelectric reflector*

Microwave devices based on ferroelectric materials are of currently attracting significant interest [21,22]. One of those typical applications is antenna beam steering by ferroelectric lens [23].

Optics EXPRESS

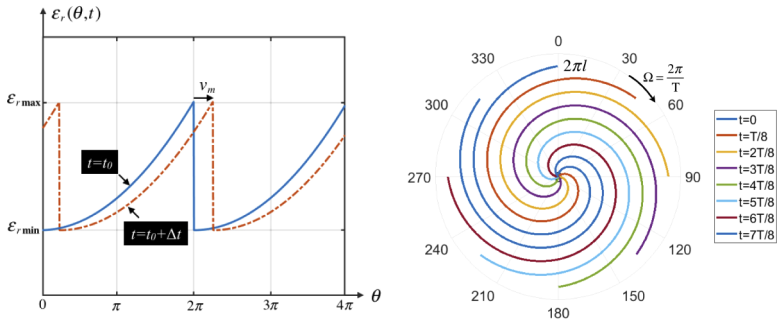

(a) (b)

Fig. 2. (a) The cylindrical spatiotemporally modulated permittivity $\epsilon_r(\theta, t)$ calculated by Eq. (3), note that the phase change is a periodic function therefore the permittivity is periodic as well. $\epsilon_{r_{min}}$ and $\epsilon_{r_{max}}$ correspond to the phase shift of 0 and $2\pi l$, respectively. v_m is the group velocity travelling in $+\theta$ direction. Two snapshots of this modulation profile are presented, demonstrating its travelling-wave character towards $+\theta$ direction. (b) Time-varying reflection phase $\varphi(\theta, t)$ profile where maximum phase change is $2\pi l$, the spinning reflection phase with an angular frequency $\Omega = 2\pi/T$ matches to the one of rotational Doppler effect from a spinning OAM beam. Eight snapshots in one period are presented to show the spinning reflection phase.

A ferroelectric lens consists of slabs of ferroelectric material sandwiched between conducting electrodes is shown in Fig. 3 on the right. The permittivity can be tuned from $\epsilon_{r_{min}}$ to $\epsilon_{r_{max}}$ by an electrostatic bias voltage. The phase of an electromagnetic wave passing through the lens can therefore be modulated by an external bias voltage. Alternatively, a reflector can be used to reflect an incident wave, and when positioned behind a ferroelectric slab with controllable permittivities, the phase of the reflected wave can be controlled. Here, a planar reflector behind ferroelectric slabs is proposed, where two Quarter-wave dielectric transformers are used for impedance matching from the vacuum to the ferroelectric material. Design details of two Quarter-wave dielectric transformers can be found in [23]. The composite bulk shown in Fig. 3 on the left is a conceptual design as the basic element of spatiotemporally modulated metamaterial. In order to obtain full 2π reflection phase tuning, the thickness of the ferroelectric material should be

$$d > \frac{\lambda}{2}(\sqrt{\epsilon_{r_{max}}} - \sqrt{\epsilon_{r_{min}}}) \tag{5}$$

One of the well-known ferroelectric materials with favorable microwave properties is barium strontium titanate (BST) [24,25]. Figure 4(a) shows the measured permittivity of $Ba_{0.6}Sr_{0.4}TiO_3$ ceramic samples at 3.5GHz vs. applied electric field. As can be seen, the dielectric constant is tunable from a value of 165 down to 120 when DC bias field is applied. It should be noted that the permittivity simulated by Vendik's model [24,25] at 10GHz has approximately the same tunability and permittivity as the one at 3.5GHz. Moreover, we simulate the permittivity and reflection phase versus bias voltage for the proposed ferroelectric reflector working at 10GHz by CST 2016, as shown in Fig. 4(a), both of which have a linear response with respect to the bias field. The loss tangent at 10GHz for different voltages are around 0.01 thus the reflection waves can be considered to have the same magnitude [26]. The detailed parameters of the full 2π reflection phase ferroelectric reflector simulation model is shown in Fig. 4(b). The permittivity of two Quarter-wave dielectric transformers are $\epsilon_1 = 5.2$ and $\epsilon_2 = 27$, respectively. There are multiple BST layers for the ferroelectric reflector, which is biased by the internal and external electrodes. The height of each layer is 1.5mm where is the space between the conducting plates.

Optics EXPRESS

This space is filled with the high dielectric constant BST and so the space is about half wavelength at 10GHz, eliminating higher order modes within the material.

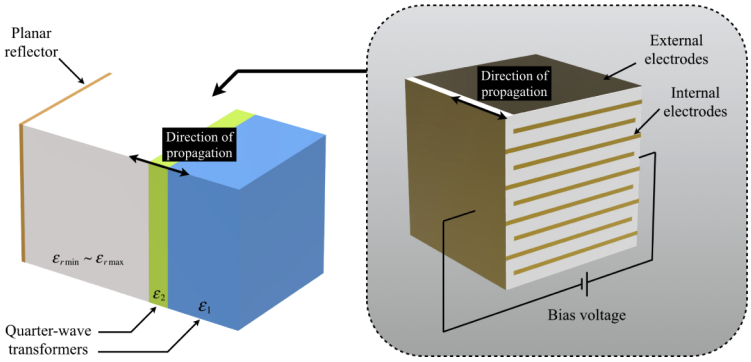

Fig. 3. Configuration of a full 2π reflection phase ferroelectric reflector. On the left is a ferroelectric bulk with planar reflector and two quarter-wave impedance transformers. The permittivity of these two quarter-wave dielectric transformer are denoted as ϵ_1 and ϵ_2, respectively. On the right is a practical configuration of a ferroelectric lens, this multilayer ferroelectric material is biased by an external voltage tuning the permittivity from $\epsilon_{r_{min}}$ to $\epsilon_{r_{max}}$.

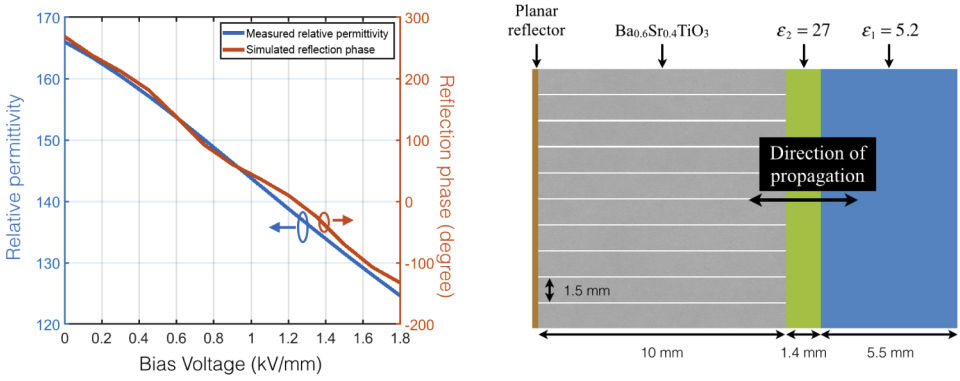

(a) (b)

Fig. 4. (a) Simulated permittivity and reflection phase versus bias voltage of the proposed ferroelectric reflector at 10 GHz, the reflection phase has a range about 400°. Measured permittivity of $Ba_{0.6}Sr_{0.4}TiO_3$ at 3.5GHz is also shown, which is the same as the permittivity at 10GHz. (b) Design details of the ferroelectric reflector working at 10GHz.

3.2. *Cylindrical spatiotemporally modulated OAM ferroelectric reflector*

A unique characteristic of an OAM beam is its helical transverse phase structure $exp(jl\theta)$, in which θ is the transverse azimuthal angle and l is an unbounded integer representing the OAM mode. An OAM beam with helical phase front can be obtained by a phase gradient material introducing azimuthal phase dependence $exp(jl\theta)$ into the beam [27–30]. In order to realize the cylindrical spatiotemporally modulated metamaterial, we need to discretize both space and time. Here we use eight elements and eight time frames to design a spatiotemporally modulated OAM ferroelectric reflector. The permittivity $\epsilon_r(\theta_N, t_M)$ of the whole reflector is changing not only

Optics EXPRESS

in azimuthal angle θ but also in time t, where $N = 1, 2, \ldots, 8$ and $M = 1, 2, \ldots, 8$, as shown in Fig. 5. The discrete spatiotemporal permittivity $\epsilon_r(\theta_N, t_M)$ is the discrete form in Fig. 2(b). Each element is a full 2π reflection phase tuning ferroelectric reflector working at 10GHz which is proposed in Fig. 4(b) and individually controlled by an external bias voltage. Specifically, we choose $l = +1$ to demonstrate the concept, but should be noted that the proposed concept can be applied in arbitrary OAM mode, the spatiotemporally modulated permittivity scheme in one period is shown in Fig. 5(b). The proposed ferroelectric reflector is consistent with the spinning helical phase condition that can generate spinning OAM reflected beam therefore causing rotational Doppler shift.

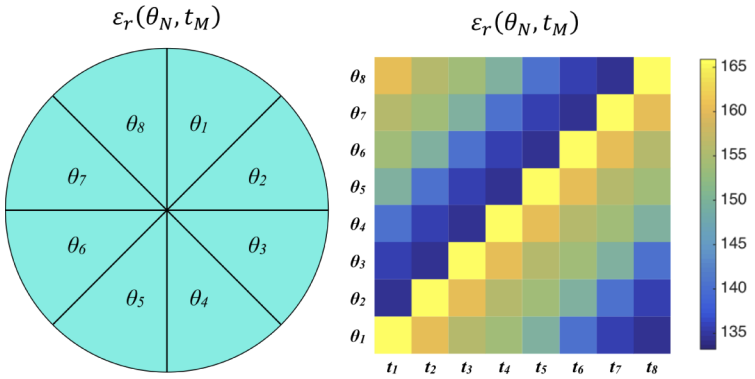

Fig. 5. (a) Structure of an OAM ferroelectric reflector. We discretize the reflector by eight elements and eight time frames to realize cylindrical spatiotemporally modulated metamaterial, each element is a full 2π reflection phase tuning ferroelectric reflector modulated by an external bias voltage. (b) Discrete spatiotemporal permittivity scheme for rotational Doppler effect of $l = +1$ OAM beam, $\theta_1 \sim \theta_8$ means different azimuthal angles, $t_1 \sim t_8$ means different time slots in one period.

From the simulated reflection phase of the proposed ferroelectric reflector, we can calculate the OAM electric field by the following Eq.

$$E(\mathbf{r}, t) = \iint_s E_0 exp(j\mathbf{k} \cdot (\mathbf{r} - \mathbf{r}_s)) exp(j\varphi(\theta, t)) ds \tag{6}$$

where $\mathbf{r}$ is the field points, $\mathbf{k}$ is the wave vector, $\mathbf{r}_s$ is the position vector on the reflector surface S, $\varphi(\theta, t)$ is the spatiotemporal reflection phase. Figure 6(b) shows the configuration of the proposed tunable OAM ferroelectric reflector for a conceptual Doppler cloak design, an object cover by the proposed reflector can get a frequency shift despite it is at rest. Figure 6(a) shows eight snapshots of the calculated spinning OAM phase front which is consistent with our theoretical results shown in Fig. 2(b). All elements can be individually modulated by applying external bias voltages in azimuthal angle and mimic the motion of spinning, where the spinning frequency is $f_m = 1/T$. Moreover, from Fig. 6(a) we can get the discrete time-varying reflection phase of the OAM beam, then we can calculate the frequency shift of an $l = +1$ wave reflected by the proposed tunable OAM ferroelectric reflector at rest, i.e., $v = 0$. By using Fourier transform $\mathcal{F}(E(\mathbf{r}, t))$ to Eq. (6), we calculate the frequency shift of a modulated signal operating at $f_0 = 10$GHz with Gaussian noise, a frequency shift $\Delta f = f_m$ is shown in Fig. 6(c). The calculated result is in a good agreement with the theoretical result $\Delta f = lf_m$. Therefore, the proposed cylindrical spatiotemporally modulated OAM ferroelectric reflector is a conceptual design for Doppler cloak by generating an opposite frequency shift related to the motion.

Optics EXPRESS

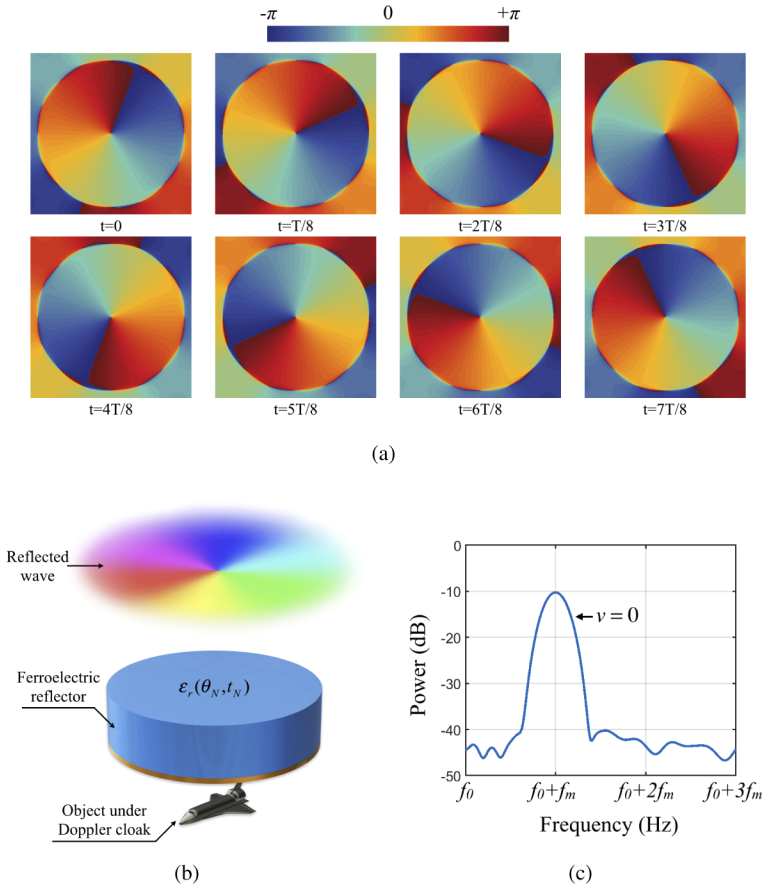

Fig. 6. (a) Calculated OAM phase front of the tunable OAM ferroelectric reflector, eight snapshots in one period, the reflection phase is spinning with time. (b) The configuration of the proposed cylindrical spatiotemporally modulated OAM ferroelectric reflector. (c) Calculated frequency shift, the signal is sinusoid with Gaussian noise then reflected by the cylindrical spatiotemporally modulated OAM ferroelectric reflector at rest.

4. Mechanical modulation: Doppler cloak by spinning OAM metasurface

As discussed above, by tuning the external voltage, we can electrically modulate the reflection phase of ferroelectric metamaterial and generate the rotational Doppler effect. Instead of electrical modulation, the spatiotemporal property can also be achieved by mechanical modulation. A more straightforward approach to modulate the reflection phase described in Eq. (1) is by physically spinning a polarization independent OAM metasurface, as a 2-dimentional spatiotemporally modulated metamaterial, which can exploit the space and time dimensions to generate rotational Doppler effect. Figure 7 shows the structure of an $l = -1$ polarization independent OAM metasurface and near-field simulated and measured phase. The near-field phase is simulated by CST 2016 and measured by a planar scanner with a 5.8-GHz Vivaldi antenna as a source.

In order to demonstrate the Doppler cloak concept, we measure the spectrogram of an OAM metasurface by a 5.8-GHz Doppler radar in three cases: moving, spinning and both moving and spinning. The experiment setup of Doppler cloak by a spinning OAM metasurface is illustrated in Fig. 8. Here we move the Doppler radar instead of the OAM metasurface to generate the relativistic movement for operational simplicity. In our measurement, the Doppler radar is moved

Optics EXPRESS

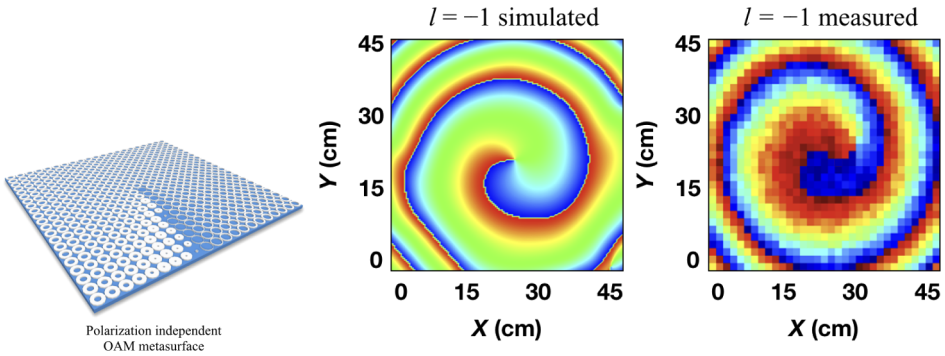

(a) (b) (c)

Fig. 7. (a) Structure of the $l = -1$ OAM metasurface. The OAM metasurface is polarization independent which can generate OAM beam in different polarizations. (b) Simulated near-field phase. (c) Measured near-field phase.

on a 2500-mm-long linear slide rail with a stepper motor and the OAM metasurface is rotated by a motor. The moving speed of the rail can be controlled by the computer which is set to $+0.62m/s$ in our case. In a radar system working at f_0, to cancel the linear Doppler shift Δf_{linear} by a rotational Doppler shift $\Delta f_{rotational}$, the relativistic moving speed v and angular velocity Ω of the OAM metasurface should satisfy the follow Eq. [31]:

$$\Delta f_{linear} + \Delta f_{rotational} = \frac{2vf_0}{c} + \frac{l\Omega}{2\pi} = 0 \tag{7}$$

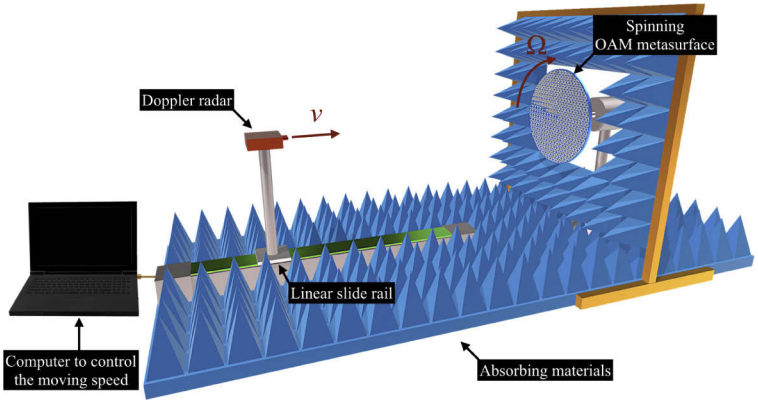

Fig. 8. Experiment of Doppler cloak by spinning OAM metasurface. A Doppler radar is moving with a linear speed and an OAM metasurface is spinning with an angular velocity, these two motions are generating a linear Doppler shift and an opposite rotational Doppler shift, respectively. Consequently, a zero-frequency shift is obtained to demonstrate the Doppler cloak concept.

The measured frequency shifts for three different cases are shown in Fig. 9. For the moving case, as shown in Fig. 9(a), a linear Doppler effect is observed. A frequency shift of +24 Hz is measured, and the output velocity, which is calculated by $v = \Delta fc/2f$ in radar system, is $+0.62m/s$. For the spinning case, as shown in Fig. 9(b), the OAM metasurface is rotated around the central axis in order to generate spatiotemporal reflection phase $\phi(\theta, t) = \theta l - 2\pi l f_m$. The OAM mode of

Optics EXPRESS

the metasurface is $l = -1$ and the angular velocity is $\Omega = 23.92 \times 2\pi rad/s$ spinning clockwise which is measured by a high-speed camera, therefore we can get a $-24Hz$ rotational Doppler shift calculated by Eq. (4). In this case, where the metasurface is spinning but not moving, and the output velocity of the radar is $-0.62m/s$. Finally, based on compensating the linear Doppler shift by an opposite rotational Doppler shift, we measure the spectrogram of an OAM metasurface that is both moving with a speed $+0.62m/s$ and spinning clockwsie with an angular velocity $\Omega = 23.92 \times 2\pi rad/s$. For normal incidence, the overall frequency shift from Eq. (7) leading to an observed zero-frequency shift and zero apparent velocity for the Doppler radar, as shown in Fig. 9(c). The measurements confirm that the spatiotemporal metasurface has the ability to cloak a moving object by generating an opposite rotational Doppler shift to the one from moving.

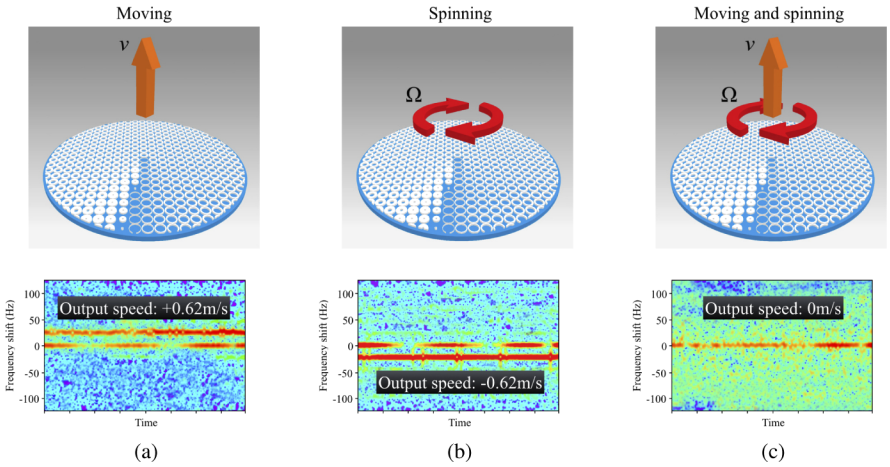

Fig. 9. Measured spectrograms of an $l = -1$ OAM metasurface in three different motions. (a) Linear moving with a speed of $+0.62m/s$, the output velocity of the Doppler radar is $+0.62m/s$. (b) Clockwise spinning with an angular velocity $\Omega = 23.92 \times 2\pi rad/s$, the output velocity of the Doppler radar is $-0.62m/s$. (c) Both moving and spinning, the overall zero-frequency shift is superposition of the linear Doppler shift and rotational Doppler shift, the output velocity of the Doppler radar is $0m/s$.

5. Conclusion

In conclusion, we have introduced an approach to generate rotational Doppler effect by cylindrical spatiotemporally modulated metamaterials. The approach is predicted by transforming the coordinate of spatiotemporally modulated metamaterial. Here we theoretically demonstrate the idea by mapping the reflection phase from a cylindrical spatiotemporally modulated metamaterial to the one of spinning OAM beam, meaning that the reflected beam from the proposed metamaterial has exactly the same characteristics of a spinning OAM beam. Moreover, we propose a conceptual design by the use of ferroelectric material and demonstrate the idea by simulation and calculation. We then discretize the device in both space and time, and an 8-element cylindrical spatiotemporally modulated array is proposed, which is termed as a voltage-controlled OAM ferroelectric reflector. Such metamaterial can be independently controlled by a field-programmable gate array (FPGA) for electronic modulation. Simulation and calculation results show that the tunable OAM ferroelectric reflector can generate a frequency shift when it is in stationary. Finally, in order to experimentally demonstrate the Doppler cloak concept by rotational Doppler effect from spatiotemporally modulated metamaterial, the spatiotemporal reflection phase is generated by a mechanical modulation. A spinning OAM metasurface with an overall zero-frequency shift by both linear and rotational Doppler shift are measured by the Doppler radar, meaning that the

Optics EXPRESS

Doppler radar cannot detect the OAM metasurface at rest despite the fact that it is moving. It should be noted that, we can arbitrarily manipulate the output velocity from a Doppler radar by tuning the spinning frequency. We only show the particular case of zero velocity in this paper. The concept of rotational Doppler effect from cylindrical spatiotemporally modulated metamaterial for Doppler cloak is introduced and demonstrated. To our knowledge, this is the first work that demonstrate the Doppler cloak concept by OAM beam experimentally, a zero-frequency shift is observed in radar system by generating an opposite rotational Doppler shift to the one of linear Doppler shift. In general, our proposed concept and design of cylindrical spatiotemporally modulated metamaterial expands the application scope of tunable metamaterials, and may find important applications to metasurface, OAM beam, Doppler radar cloaking, radar deception and Doppler cancellation in wireless mobile communications. The proposed concept can also be extended to millmeter-wave or optical ranges, as well as to acoustic waves by spatiotemporally modulating corresponding properties of the medium.

Funding

Natural Science Foundation of Guangdong Province (2018A030313481); Shenzhen University Research Startup Project of New Staff (20188082); Engineering and Physical Sciences Research Council (EP/N010493/1, EP/R035393/1); National Natural Science Foundation of China (61871194); Shenzhen Science and Technology Programs (GJHZ 20180418190529516, JCYJ 20180305124543176, JSGG 20180507183215520).

Disclosures

The authors declare no conflicts of interest.

References

1. R. Liu, C. Ji, J. Mock, J. Chin, T. Cui, and D. Smith, "Broadband ground-plane cloak," Science **323**(5912), 366–369 (2009).
2. W. Cai, U. K. Chettiar, A. V. Kildishev, and V. M. Shalaev, "Optical cloaking with metamaterials," Nat. Photonics **1**(4), 224–227 (2007).
3. J. B. Pendry, D. Schurig, and D. R. Smith, "Controlling electromagnetic fields," Science **312**(5781), 1780–1782 (2006).
4. H. Chen, C. T. Chan, and P. Sheng, "Transformation optics and metamaterials," Nat. Mater. **9**(5), 387–396 (2010).
5. J. C. Halimeh, R. T. Thompson, and M. Wegener, "Invisibility cloaks in relativistic motion," Phys. Rev. A **93**(1), 013850 (2016).
6. D. Ramaccia, D. L. Sounas, A. Alù, A. Toscano, and F. Bilotti, "Doppler cloak restores invisibility to objects in relativistic motion," Phys. Rev. B **95**(7), 075113 (2017).
7. D. Ramaccia, A. Toscano, F. Bilotti, D. Sounas, and A. Alù, "Time-modulated reflective metasurface for the control of the reflected signal frequency," in *2019 IEEE International Symposium on Antennas and Propagation and USNC-URSI Radio Science Meeting*, (IEEE, 2019), pp. 1611–1612.
8. D. Ramaccia, D. L. Sounas, A. Alù, A. Toscano, and F. Bilotti, "Frequency-shifted reflection achieved through time-varying metasurfaces," in *2019 Thirteenth International Congress on Artificial Materials for Novel Wave Phenomena (Metamaterials)*, (IEEE, 2019), pp. 327–329.
9. D. Ramaccia, D. L. Sounas, A. Alù, A. Toscano, and F. Bilotti, "Phase-induced frequency conversion and doppler effect with time-modulated metasurfaces," *IEEE Transactions on Antennas and Propagation* pp. 1–11 (2019).
10. M. P. Lavery, F. C. Speirits, S. M. Barnett, and M. J. Padgett, "Detection of a spinning object using light's orbital angular momentum," Science **341**(6145), 537–540 (2013).
11. O. Korech, U. Steinitz, R. J. Gordon, I. S. Averbukh, and Y. Prior, "Observing molecular spinning via the rotational doppler effect," Nat. Photonics **7**(9), 711–714 (2013).
12. G. Li, T. Zentgraf, and S. Zhang, "Rotational doppler effect in nonlinear optics," Nat. Phys. **12**(8), 736–740 (2016).
13. H. Zhou, D. Fu, J. Dong, P. Zhang, and X. Zhang, "Theoretical analysis and experimental verification on optical rotational doppler effect," Opt. Express **24**(9), 10050–10056 (2016).
14. K. F. Li, J. H. Deng, X. Liu, and G. Li, "Observation of rotational doppler effect in second harmonic generation in reflection mode," Laser Photonics Rev. **12**(7), 1700204 (2018).
15. Y. Li, X. Li, L. Chen, M. Pu, J. Jin, M. Hong, and X. Luo, "Orbital angular momentum multiplexing and demultiplexing by a single metasurface," Adv. Opt. Mater. **5**(2), 1600502 (2017).

Optics EXPRESS

16. B. Liu, H. Chu, H. Giddens, R. Li, and Y. Hao, "Experimental observation of linear and rotational doppler shifts from several designer surfaces," Sci. Rep. **9**(1), 8971 (2019).
17. P. Georgi, C. Schlickriede, G. Li, S. Zhang, and T. Zentgraf, "Rotational doppler shift induced by spin-orbit coupling of light at spinning metasurfaces," Optica **4**(8), 1000–1005 (2017).
18. A. Tennant and B. Allen, "Generation of oam radio waves using circular time-switched array antenna," Electron. Lett. **48**(21), 1365–1366 (2012).
19. L. Zhang, X. Q. Chen, S. Liu, Q. Zhang, J. Zhao, J. Y. Dai, G. D. Bai, X. Wan, Q. Cheng, G. Castaldi, G. Vincenzo, and T. J. Cui, "Space-time-coding digital metasurfaces," Nat. Commun. **9**(1), 4334 (2018).
20. D. Ramaccia, D. L. Sounas, A. Alù, F. Bilotti, and A. Toscano, "Nonreciprocity in antenna radiation induced by space-time varying metamaterial cloaks," Antennas Wirel. Propag. Lett. **17**(11), 1968–1972 (2018).
21. L. W. Martin and A. M. Rappe, "Thin-film ferroelectric materials and their applications," Nat. Rev. Mater. **2**(2), 16087 (2017).
22. A. Ahmed, I. A. Goldthorpe, and A. K. Khandani, "Electrically tunable materials for microwave applications," Appl. Phys. Rev. **2**(1), 011302 (2015).
23. J. B. Rao, D. P. Patel, and V. Krichevsky, "Voltage-controlled ferroelectric lens phased arrays," IEEE Trans. Antennas Propag. **47**(3), 458–468 (1999).
24. A. Feteira, D. C. Sinclair, I. M. Reaney, Y. Somiya, and M. T. Lanagan, "Batio3-based ceramics for tunable microwave applications," J. Am. Ceram. Soc. **87**(6), 1082–1087 (2004).
25. O. Vendik, S. Zubko, and M. Nikolski, "Microwave loss-factor of Ba x Sr 1-x Tio 3 as a function of temperature, biasing field, barium concentration, and frequency," J. Appl. Phys. **92**(12), 7448–7452 (2002).
26. L. C. Sengupta and S. Sengupta, "Breakthrough advances in low loss, tunable dielectric materials," Mater. Res. Innovations **2**(5), 278–282 (1999).
27. A. M. Yao and M. J. Padgett, "Orbital angular momentum: origins, behavior and applications," Adv. Opt. Photonics **3**(2), 161–204 (2011).
28. B. Thidé, H. Then, J. Sjöholm, K. Palmer, J. Bergman, T. Carozzi, Y. N. Istomin, N. Ibragimov, and R. Khamitova, "Utilization of photon orbital angular momentum in the low-frequency radio domain," Phys. Rev. Lett. **99**(8), 087701 (2007).
29. B. Liu, Y. Cui, and R. Li, "A broadband dual-polarized dual-oam-mode antenna array for oam communication," Antennas Wirel. Propag. Lett. **16**, 744–747 (2017).
30. B. Liu, G. Lin, Y. Cui, and R. Li, "An orbital angular momentum (oam) mode reconfigurable antenna for channel capacity improvement and digital data encoding," Sci. Rep. **7**(1), 9852 (2017).
31. L. Fang, M. J. Padgett, and J. Wang, "Sharing a common origin between the rotational and linear doppler effects," Laser Photonics Rev. **11**(6), 1700183 (2017).